

Impact of Horizontal and Vertical Heterogeneities on Retrievals Using Multiangle Microwave Brightness Temperature Data

Eleanor J. Burke, W. James Shuttleworth, and Paul R. Houser

Abstract—This paper investigates the impact of heterogeneity at the land surface on geophysical parameters retrieved from multiangle microwave brightness temperature data, such as would be obtained from the Soil Moisture and Ocean Salinity (SMOS) mission. Synthetic brightness temperature data were created using the Common Land (land surface) Model, coupled with a microwave emission model and set within the framework of the North American Land Data Assimilation System (NLDAS). Soil moisture, vegetation optical depth, and effective physical temperature were retrieved using a multiobjective calibration routine similar to the proposed SMOS retrieval algorithm for a typical on-axis range of look angles. The impact of heterogeneity both in the near-surface profiles of soil moisture and temperature and in the land cover on the accuracy of the retrievals was examined. There are significant errors in the retrieved parameters over regions with steep gradients in the near-surface soil moisture profile. These errors are approximately proportional to the difference in the soil water content between the top (at 0.7 cm) and second layer (at 2.7 cm) of the land surface model. The errors resulting from heterogeneity in the land cover are smaller and increase nonlinearly with increasing land-surface heterogeneity (represented by the standard deviation of the optical depth within the pixel). The most likely use of retrieved soil moisture is through assimilation into an LDAS for improved initiation of weather and climate models. Given that information on the soil moisture profile is already available within the LDAS, the error in the retrieved soil moisture as a result of the near-surface profile can be corrected for. The potential errors as a result of land-surface heterogeneity can also be assessed for use in the assimilation process.

Index Terms—Land surface, passive microwave, remote sensing, retrieval, soil moisture.

I. INTRODUCTION

THERE IS NOW ample evidence that, over continental areas, weather and climate are significantly influenced by the local and regional availability of soil moisture that can reach the atmosphere by evaporation from soil or by transpiration from plants (e.g., [1]–[4]). At least at midlatitudes, and at least during the warm season, weather and climate forecasts can be improved by providing better initiation and description of the

subsequent evolution of soil-moisture status in forecast models. At present, the most practical method is via the use of land data assimilation systems (LDAS). LDAS are two-dimensional arrays of the land-surface scheme of the relevant weather or climate forecast model, e.g., see <http://ldas.gsfc.nasa.gov>. These land-surface schemes are forced mainly by observations, so the soil moisture status is not biased by poor estimation of the near-surface atmospheric forcing, especially precipitation. It is possible that LDAS will become the routine mechanism by which many predictive weather and climate models will be initiated in coming years. Assuming this is so, it will be via assimilation into LDAS that other data relevant to the current status of the land surface, such as remotely sensed estimates of soil moisture, will find value for initiating predictive models.

It is well established that passive microwave radiometers operating at 1.4 GHz have the potential to estimate the near-surface soil moisture [5]–[7]. Over the past years, there have been many experiments using truck- and aircraft-based radiometers to explore the relationship between microwave brightness temperature and near-surface soil moisture [6], [8]. Satellite-based large-scale estimates of soil moisture using L-band microwave brightness temperatures are likely to become available over the next five years. For example, the Soil Moisture and Ocean Salinity (SMOS) mission is planned for launch in ~2007 [9]. This consists of a dual-polarized two-dimensional aperture synthesis radiometer that will measure microwave brightness temperatures at multiple look angles over almost the same location at a resolution ~50 km. At this scale, there is likely to be large within-pixel variability. However, one of the assumptions implicit in any proposed retrieval algorithm is that the land surface is homogeneous. There have been several studies where the impact of heterogeneity in land cover has been evaluated. Drusch *et al.* [10], Liou *et al.* [11], and Crow *et al.* [12] all used synthetically generated low-frequency microwave brightness temperatures to evaluate the effects of subpixel heterogeneity on the retrieved soil moisture and suggest that errors are generally less than $0.03 \text{ cm}^3 \cdot \text{cm}^{-3}$. However, Van de Griend *et al.* [13] suggest that under certain circumstances the errors can be more significant.

This paper explores the impact of land-surface heterogeneity on the accuracy of the retrieved parameters using synthetic microwave brightness temperatures generated for North America for a set of typical on-axis look angles proposed for SMOS. It considers in detail the relative impact of two types of heterogeneity: 1) shape of the near-surface profile of soil temperature and soil water content and 2) presence of different land covers

Manuscript received November 18, 2003; revised February 2, 2004. The work was supported by the National Aeronautics and Space Administration under Contract NAG5-8214.

E. J. Burke and W. J. Shuttleworth are with the Department of Hydrology and Water Resources, University of Arizona, Tucson, AZ 85721 USA (e-mail: eleanor@hwr.arizona.edu).

P. R. Houser is with Hydrological Sciences Branch, NASA Goddard Space Flight Center, Greenbelt, MD 20771 USA.

Digital Object Identifier 10.1109/TGRS.2004.828922

within the pixel. It concludes with a discussion of the value of the retrieved soil moisture for assimilation into an LDAS.

II. MODELS

A. Land Surface Model

The land surface model used in this study is the Common Land Model (CLM). CLM [14] includes the best elements of some well-tested physical parameterizations and numerical schemes (e.g., the National Center for Atmospheric Research Land Surface Model (LSM) [15], Biosphere–Atmosphere Transfer Scheme (BATS) [16], and the Institute of Atmospheric Physics Land Surface Model (IAP94) [17]). It requires a set of parameters that specify physical constants and aspects of the soil and vegetation, and given meteorological forcing variables, it then provides prognostic and diagnostic land-surface state variables and surface energy and water fluxes as output. CLM describes the diffusion of soil heat and liquid water through several (typically ten) layers of soil using the finite-difference form of the thermal diffusion equation and Richard's equation, respectively. CLM uses the fraction of sand and clay to specify the properties of the soil. If vegetation is present, it is represented as though it is at a single level, at the height $(d + z_0)$, where d is the zero plane displacement, and z_0 is the aerodynamic roughness of the canopy. Turbulent transport between this level and a specified reference height above the canopy is described using the Monin–Obukhov similarity theory, with allowance made for the effect of atmospheric stability. The whole canopy surface resistance is parameterized following the model introduced by [18].

In this study, CLM was run in the framework of the NLDAS. This consists of several physically based land-surface models running in near real time, on a common 0.125° grid covering the contiguous United States, driven by common surface forcing fields. The forcing fields are characterized by observed, hourly, gauge/radar precipitation and observed Geostationary Operational Environmental Satellite-based satellite-derived surface solar insolation. The remainders of the surface-forcing data are interpolated from the 3-h 40-km Eta Data Assimilation System analysis carried out by the National Centers for Environmental Prediction. The common land-surface parameters (including vegetation type, soil type, and topography) were defined from high-resolution (typically 1 km) datasets [19]. Subgrid-scale heterogeneity is incorporated within CLM by subdividing each grid into a mosaic of tiles, with each tile having its own vegetation type and hence water and energy balance.

B. Microwave Emission Model

The profiles of soil temperature and soil water content calculated by the CLM are required by the microwave emission model. The ten layers used in CLM were at depths of 0.7, 2.7, 6.2, 11.9, 21.2, 36.6, 61.9, 100.4, 172.7, and 286.4 cm. Following [8] and [20], a linear interpolation procedure was used to interpolate these depths to the following thicknesses and depths: 0–1 cm, ten layers at 1 mm; 1–3 cm, ten layers at 2 mm; 3–6 cm, ten layers at 3 mm; 6–10 cm, ten layers at 4 mm; 10–20 cm, 20 layers at 5 mm; and 20–160 cm, 140 layers at 10 mm. This

profile soil water content was then used to estimate the soil profile dielectric permittivity using the Dobson *et al.* [21] model. The profiles of dielectric permittivity and soil temperature were then used by the Wilheit [22] model of coherent emission from a stratified medium to calculate the emission at the soil surface. For simplicity, in this analysis, any impact of topography, ice, snow, or soil surface roughness on the microwave brightness temperature was assumed to be negligible.

A vegetation canopy will scatter and absorb microwave emission from the soil. It will also contribute with its own emission, which will be scattered and absorbed by the canopy through which it passes. A simple model was used to account for the effects of vegetation on microwave emission from the soil [23]

$$T_B = \Gamma T_{B\text{soil}} + (1 - \Gamma)T(1 + \Gamma r_s) \quad (1)$$

where T_B is the microwave brightness temperature above the canopy, $T_{B\text{soil}}$ is the microwave brightness temperature at the soil surface, Γ is the transmissivity of the vegetation layer, and r_s is the reflectivity of the soil surface (for the purposes of this paper, the single-scattering albedo is assumed to be zero). The transmissivity (Γ) of the vegetation layer is related to the optical depth (τ) by

$$\Gamma = e^{-\tau \sec \phi} \quad (2)$$

where ϕ is the look angle. The optical depth defines the amount of absorption by the canopy and is often, for a specified vegetation type and frequency [24], taken to be proportional to the vegetation water content.

C. Retrieval Algorithm

The retrieval algorithm used in this study mimics that proposed for the SMOS mission [7] and delivers three variables over land surfaces, namely, near-surface soil moisture, the optical depth of the vegetation cover, and the effective temperature of the land surface. The retrieval algorithm is also based on a forward calculation of microwave brightness temperature. The Fresnel model describes the microwave emission from the soil surface and assumes that the soil is a semi-infinite uniform slab of dielectric material. As in the initial calculation of microwave brightness temperature, the soil dielectric was calculated using Dobson's [21] model, and the simple model of Jackson and Schmugge [23] was used to describe the effect of vegetation on the emission from the soil. Therefore, in this study, the only difference between the initial calculation of microwave emission and the retrieval algorithm is the description of the soil profile. In the initial calculation, realistic vertical profiles were used, while in the retrieval uniform vertical profiles of soil moisture and temperature were assumed. Despite different methodologies being used to calculate the emission at the soil surface, if a uniform soil temperature and water content profile is assumed, the microwave brightness temperature is independent of whether it is calculated by the Fresnel model or by the Wilheit [22] model.

The SMOS mission will provide observations of surface brightness temperatures at several angles for each point on the ground, the number and selection of angles depending on the location of the point within the sensor footprint (see <http://www.esa.int/esaLP/smos.html>). The retrieval algorithm uses multiparameter optimization techniques to minimize

the difference between modeled and measured microwave brightness temperature for the available range of look angles and polarizations. The optimization algorithm used in this paper is the Shuffled Complex Evolution algorithm (SCE-UA) [25]. The SCE algorithm has good convergence properties over a broad range of problems and a high probability of succeeding in its objective of finding the global optimum [25].

III. METHODOLOGY

Synthetic SMOS microwave brightness temperatures distributed over North America were created within the framework of the LDAS using the coupled CLM and the microwave emission model described above. The synthetic brightness temperatures were created at both horizontal and vertical polarization for a typical on-axis pixel, where the range of look angles is greatest. In this study, there were 41 look angles simulated ranging from 0° to 55° . For the purposes of this paper, it was assumed that (2) adequately describes the transmissivity as a function of look angle.

CLM was parameterized and forced using the standard LDAS framework [19]. Soil type was available at the 0.125° grid, and vegetation type was available at 1-km resolution. In the case of the microwave emission model, the parameterization of the optical depth was undefined by the LDAS framework. A commonly used line of attack is to define the constant of proportionality in the relationship between optical depth and vegetation water content [23] for each class of vegetation within a land-cover classification and to use vegetation indices derived from visible/near-infrared satellite data to estimate the amount of vegetation present, but there are few studies of the accuracy of estimating vegetation optical depth in this way [24]. In general, little is known about the global distribution of optical depth [26]. For the purposes of this study, it is sufficient to define the optical depth using the land cover classification and typical assumed values for the vegetation water content within these classes as in [26].

Synthetic brightness temperatures were calculated for three scenarios. The first scenario (A) explores the impact of the nonuniform profile of soil moisture and soil temperature on the retrieved parameters. In this example, the LDAS was run by assuming one patch of vegetation and one soil type per LDAS grid; representing the dominant land cover type within that grid. It was spun up for one year, and then, synthetic brightness temperatures were created for July 1, 1997, at 12:00 UTC. This represents a local time of between 4 A.M. and 7 A.M. depending on the location within the continental U.S. For this example the synthetic pixels were assumed to be identical in size to one LDAS grid (a resolution of 0.125°). Since the land cover is taken to be homogeneous over the grid cell, the size of the grids is not significant, and in fact, the use of more cells increases the amount of data available for statistical analysis.

The second scenario (B) explores the impact of heterogeneity at the land surface on the accuracy of the retrieved parameters. In this example the soil moisture profile was assumed to be uniform and taken to be equal to the mean top 5-cm soil moisture calculated by CLM. The soil temperature profile was also assumed to be uniform and set to the CLM-calculated value at

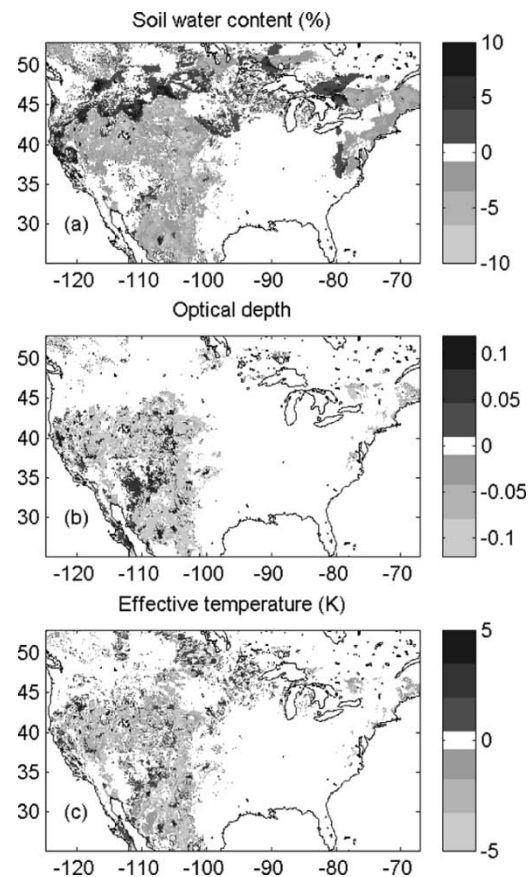


Fig. 1. Distribution of errors (retrieved—expected) in the retrieved (a) soil moisture (percent), (b) optical depth, and (c) effective temperature (Kelvin) over the NLDAS domain. Profile information in the soil temperature and soil water content were included in the synthetically generated brightness temperatures.

6.2 cm. In this scenario, to obtain realistic estimates of heterogeneity, the pixel size was set to be similar to the size of the proposed SMOS pixels. The soil type was set to the dominant value within each pixel. CLM was run in mosaic form, and up to eight patches of vegetation per grid cell were included. Microwave brightness temperatures were calculated for 0.5° grids (~ 48 km). This is an interesting scenario because it includes the relative interactions of soil and vegetation, which was not accounted for by [13] or [27].

The third scenario (C) explores the interactions of the impact of both vertical and horizontal heterogeneity on the retrieved parameters. The brightness temperatures were calculated for the 0.5° grids as in Scenario B. However, for each tile the shape of the profile in soil water content and soil temperature was included during the calculation of brightness temperature. An assumed measurement error in the microwave brightness temperature was included in the calculation of the synthetic measurements. This was done by adding a random error with a standard deviation of 1 K to each brightness temperature synthesized. One hundred sets of synthetic brightness temperatures (each set containing 41 brightness temperatures at the 41 different look angles) were created and the soil moisture, vegetation optical depth and effective temperature retrieved for each set.

It was assumed that retrievals could be made over the entire LDAS domain. However, in reality, areas of topography, snow

TABLE I
PERCENTAGE AREA, FOR WHICH THERE IS ERROR, AND THE RMSE AND BIAS OF THAT ERROR FOR RETRIEVED VALUES OF THE MEAN TOP 5-cm SOIL WATER CONTENT, THE OPTICAL DEPTH, AND THE EFFECTIVE TEMPERATURE

Scenario	Error in water content, θ ($>0.5\%$)			Error in optical depth, τ (>0.03)			Error in effective temp, T_{eff} ($>0.8K$)		
	Area (%)	RMSE (%)	Bias (%)	Area (%)	RMSE	Bias	Area (%)	RMSE (K)	Bias (K)
A (profile T & θ)	50.7	3.8	-0.9	21.0	0.11	-0.05	24.6	2.6	-1.1
A (uniform θ & profile T)	2.8	0.7	0.7	3.7	0.05	0.05	1.6	0.9	0.9
A (uniform T & profile θ)	50.0	3.9	-1.2	20.1	0.12	-0.08	24.7	2.7	-1.5
B	54.6	1.5	-1.3	37.1	0.06	-0.05	46.1	1.6	-1.4
C	78.0	2.9	-1.7	47.5	0.08	-0.07	54.5	2.2	-1.8

cover, etc., will exist and make retrievals inaccurate over those locations. The retrieval assumes that the soil water content and temperature profiles and the land cover are uniform within a pixel. This methodology provides an opportunity to explore the impact of land-surface heterogeneity on retrievals of geophysical parameters.

IV. RESULTS

A. Scenario A—Impact of Slope of Near-Surface Soil Profile

Fig. 1 shows the magnitude and distribution of the errors in the retrieved parameters at a 0.125° resolution. The retrieved temperature is compared to the effective temperature modeled by the Wilheit [22] model and the soil moisture is compared to the mean soil moisture in the top 5 cm modeled using CLM. Errors are solely a result of the shape of the profiles of soil moisture and soil temperature. They are mainly located in southwestern United States, where it is semiarid. In these locations, they are potentially serious. On average, for locations where there are errors, the root mean squared error (RMSE) between the retrieved and true parameters are 3.8%, 0.11, and 2.6 K for soil moisture, vegetation optical depth, and effective temperature, respectively (Table I). Fig. 1 indicates that the errors represent a combination of both over- and underestimation by the retrievals. However, on average, the retrieved values are slightly less than the expected values (Table I). The relative impacts of the shape in the soil water content and soil temperature profiles on these errors were then explored.

Scenario A was repeated using profile information in either soil water content or soil temperature. Table I shows that errors as a result of including only the profile information in soil temperature cover an area of around 1% to 4% of the LDAS domain and their magnitudes are small. However, errors as a result of including profile information in soil water content cover approximately the same proportion of the LDAS domain as in Scenario A and are of similar magnitude (Table I). Therefore, the shape of the profile in the soil water content is the most significant contributor to the error in Scenario A. This was explored further by comparing the near-surface gradient of the CLM-modeled soil moisture with the magnitude of the error.

Fig. 2 shows there is a strong correlation between the difference in the CLM-modeled soil moisture in layer 1 (at 0.7 cm) and that in layer 2 (at 2.6 cm) and the error in the retrieved soil moisture. As a general rule, the retrieved soil moisture is over estimated when the surface soil moisture layer is wetter than the deeper soil moisture layer and vice versa. This might be expected, because the Wilheit [22] model gives the emission

from nearer the surface a greater weight than the emission from deeper in the soil profile, whereas the Fresnel model just assumes a uniform profile. Fig. 2 shows the linear fit through this relationship with an R^2 value of 83.9%. Scatter around this fit is mainly a result of contribution to the microwave brightness temperature from deeper within the soil.

B. Scenario B—Impact of Heterogeneity in Land Cover

Fig. 3 shows the magnitude and distribution of the errors in the retrieved parameters at 0.5° resolution. In this case, the profiles of soil moisture and temperature were assumed to be uniform, and assigned to vegetation-type-specific values. Therefore, any errors are solely a result of within-pixel differences in the land cover type. The retrieved soil moisture and temperature were then compared with the area-weighted values of the soil moisture and temperature. Since it is transmissivity and not optical depth that scales linearly, the retrieved optical depth was compared to the optical depth found from the area weighted average transmissivity calculated at 0° look angle using (1). The errors (Fig. 3) are distributed over the entire LDAS domain. In addition, they cover a larger proportion of the domain than in Scenario A. However, in locations where there are errors, the magnitudes are about half the magnitudes of the errors for Scenario A (Table I). In general, the retrieved parameters are less than the actual values, with the bias being of the same order as the RMSE. The impact of the degree of heterogeneity on these errors was explored.

The degree of heterogeneity at the land surface is represented by the standard deviation of the optical depth within the pixel. Fig. 4 shows that the magnitude of the error in both retrieved soil water content and optical depth increases with increasing standard deviation. In the case of optical depth, there is a predictable relationship between the error and the degree of heterogeneity. The exponential fit through the relationship has an R^2 value of 70.4%. In the case of soil moisture, the relationship is less predictable: the exponential fit through this relationship has an R^2 value of only 37.9%. There is, however, a general trend of increasing maximum error with increasing standard deviation of optical depth. There is no apparent relationship between the error in retrieved effective temperature and degree of heterogeneity (not shown).

C. Scenario C—Impact of Heterogeneity at the Land Surface

Fig. 5 shows the error in the retrieved parameters when both the shape of the profile in the soil moisture and soil temperature and the heterogeneity in the land cover are included. The parameters are retrieved for a 0.5° grid as in Scenario B. The top

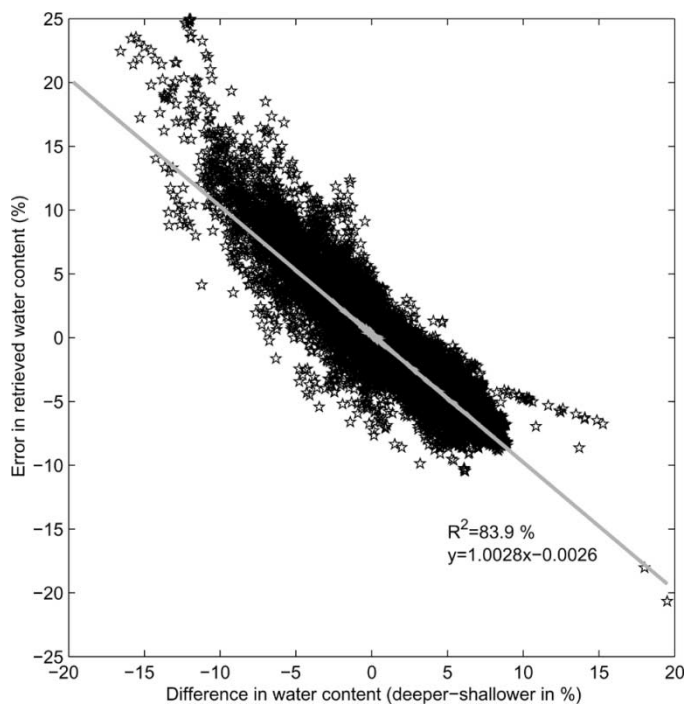


Fig. 2. Relationship between the difference in the two top layers of the CLM-modeled water content and the error in the retrieved soil moisture (retrieved—expected).

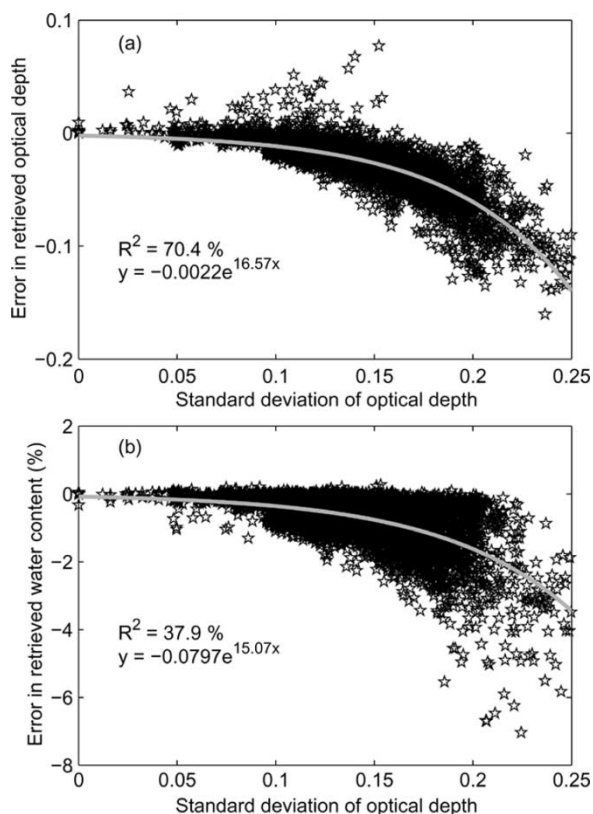


Fig. 4. Relationship between land-cover heterogeneity, represented in this case by the standard deviation of the optical depth, and the error in retrieved (a) optical depth and (b) soil moisture (percent).

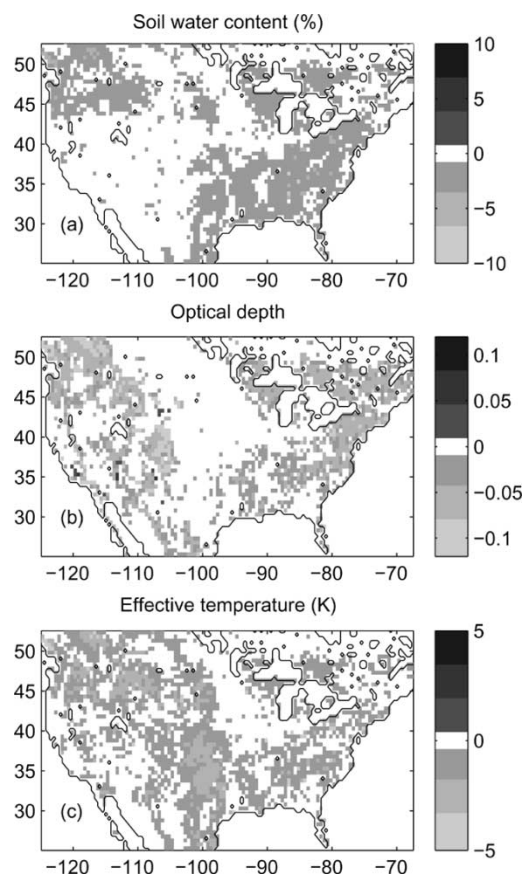


Fig. 3. Distribution of errors (retrieved—expected) in the retrieved (a) soil moisture (percent), (b) optical depth, and (c) effective temperature (Kelvin) over the NLDAS domain. Heterogeneity in the land cover was included in the synthetically generated brightness temperatures.

row of figures shows the mean error for the 100 sets of brightness temperatures. There are errors in the retrieved soil water content for the majority of the land area (Table I). These errors are negative for the majority of the cells. The RMSE of 2.9% between the expected and retrieved soil water content is significant considering that, in reality, there will be additional contributing factors. The additional contribution of any instrumental errors in the measurement of the brightness temperature was explored by adding a different random error to each synthetic brightness temperature measurement. The standard deviation of the error in the retrieved parameters is shown in the bottom row of figures in Fig. 5. There is, on average, between 0.5 and 1% by volume standard deviation in the errors of the retrieved soil water content. This could result in up to 1% to 2% by volume additional error in the retrieved soil water content. The standard deviation of the error in the retrieved optical depth is small over the majority of the LDAS domain. However, in the semiarid southwest, the standard deviations increase to ~ 0.05 and greater.

V. VALUE OF DATA FOR ASSIMILATION INTO LAND SURFACE MODELS

The most likely use of low-resolution microwave brightness temperatures from missions such as SMOS, will be via assimilation within an LDAS framework for improved soil-moisture initialization of weather and climate models. Therefore, there is information already present within the LDAS, which can be incorporated into the soil moisture retrieval algorithm both to

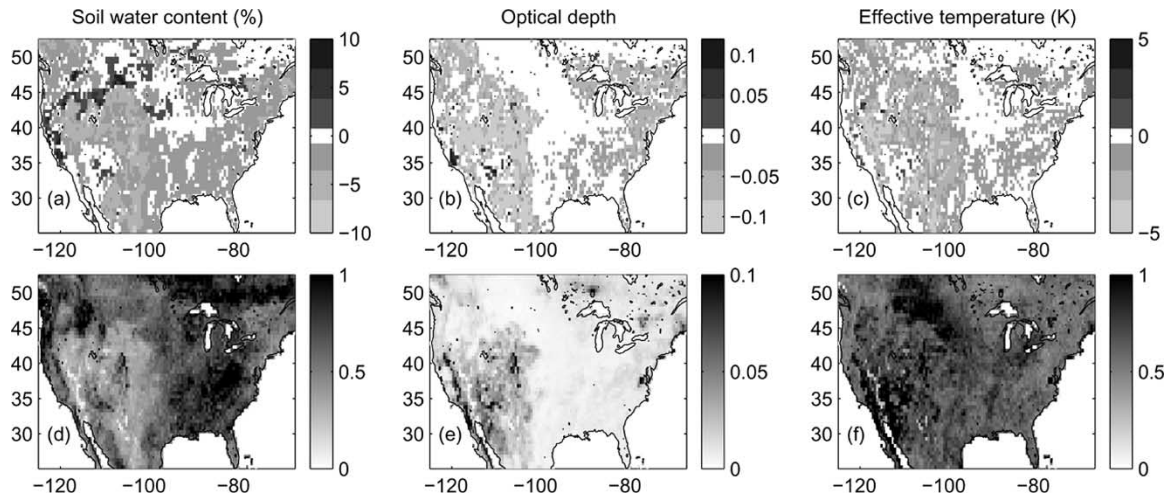


Fig. 5. Mean error in retrieved (a) soil moisture (percent), (b) optical depth, and (c) effective temperature (Kelvin) resulting from both the shape of the soil moisture profile and the degree of land-surface heterogeneity. Standard deviation of the error in the retrieved (d) soil moisture (percent), (e) optical depth, and (f) effective temperature (Kelvin) from the sample of 100 sets of synthetic microwave brightness temperatures.

improve the accuracy of the retrieved soil moisture and to quantify the errors.

It has been shown that there are errors in the retrieved soil moisture introduced as a result of near-surface gradients in soil moisture. However, there is a strong relationship between the slope of the near-surface soil moisture profile and the errors (Fig. 2). An LDAS will provide information on the slope of the near-surface soil moisture profile, which can then be used, in conjunction with such a relationship to correct for these errors. This relationship will be model specific. However, this specificity is a cause for concern that is already present within the LDAS approach itself. The equation shown in Fig. 2 was used to correct for errors in the retrieved soil moisture in Scenario A. This resulted in a reduction of the proportion of the domain with error as well as a reduction in the bias and magnitude.

A 1-km land cover classification can be used to estimate the degree of heterogeneity of the land cover within the LDAS. In scenario B, the relationship shown in Fig. 4(b) was used to correct for a bias in the retrieved soil moisture. This had little effect on the RMSE because the fit is relatively poor. However, the mean bias across the LDAS domain was corrected from -1.2% to 0% (Table II). This correction also resulted in a reduction in the proportion of the domain over which there are errors.

Both of the above correction factors can be used in conjunction with Scenario C. After correction, there are errors over 44.3% of the domain (compared to 78% previously). The RMSE and bias are reduced from 2.9% and -1.7% to 1.6% and 0.4% respectively. This represents a significant improvement. As expected the correction for the profile soil moisture has a greater impact on the accuracy of the retrieved soil moisture than the correction for land-surface heterogeneity (Table II).

An assessment of the potential errors in the retrieved soil moisture is also valuable in the assimilation process. Even though the errors shown in Figs. 1 and 3 cannot be totally corrected for, the quality of the fits shown in Figs. 2 and 4 can be used to provide an estimate of the potential error. This potential error can then be used to weight the soil moisture

TABLE II
PERCENTAGE AREA, FOR WHICH THERE IS ERROR, AND THE RMSE AND BIAS OF THAT ERROR FOR RETRIEVED VALUES OF THE MEAN TOP 5-CM SOIL WATER CONTENT AFTER BEING CORRECTED FOR THE IMPACTS OF HETEROGENEITY AT THE LAND SURFACE

Scenario Corrected	Area (%)	RMSE (%)	Bias (%)
A (profile T & θ)	33.3	2.1	0.2
B	33.0	1.0	-0.0
C (correcting using land-cover heterogeneity)	63.6	2.7	-0.8
C (correcting using profile information)	52.4	1.7	-0.8
C (correcting using both profile information and land-cover heterogeneity)	44.3	1.6	0.4

appropriately during the assimilation process. In the case of the profile information in soil moisture, the errors are relatively independent of the shape of the profile (Fig. 2). However, in the case of land-cover heterogeneity (Fig. 4), the errors are a function of the degree of heterogeneity. For example, with a standard deviation of the optical depth equal to 0.1, the maximum error in the soil water content is $\pm 0.5\%$, and when the standard deviation is 0.2, the maximum error is $\pm 1.5\%$.

VI. CONCLUSION

This paper discusses the impacts of heterogeneity at the land surface on the accuracy of retrieved soil moisture, vegetation optical depth, and soil effective temperature, given multiangle brightness temperature information. Retrievals are performed on a synthetically simulated set of microwave brightness temperatures over North America.

When information on the shapes of the profiles of soil temperature and soil water content was included within the calculation of the synthetic microwave brightness temperatures, there were significant errors in the retrieved parameters mainly over the southwestern United States. These errors were found to be a function of the gradient of the near-surface soil water content. When information on subpixel land-surface heterogeneity was included within the calculation of the synthetic microwave brightness temperatures, there are errors for $\sim 50\%$ of the area. In nearly all of the pixels for which there are

errors, the retrieved parameters are less than the expected parameters. The potential magnitude of the errors increases with increasing degree of heterogeneity.

The retrieved soil moisture is likely to be used via assimilation into a land-surface model within an LDAS framework. Therefore, there is information already present in the LDAS, which can be used to help correct for errors in the retrieved soil moisture resulting from land-surface heterogeneity and the shape of the near-surface soil moisture profile, specifically a high-resolution land-cover classification or simulated profiles of soil moisture. Knowledge of the potential errors in the retrieved soil moisture can be used to give value to the retrieved soil moisture to be assimilated. This study focuses on one time period over North America. In order to develop a methodology for satellite-derived soil moisture assimilation, the impact of climate on the errors in the retrieved soil moisture needs to be fully assessed.

REFERENCES

- [1] A. K. Betts, J. H. Ball, A. C. M. Beljaars, M. J. Miller, and P. Viterbo, "The land-surface-atmosphere interaction: A review based on observational and global modeling perspectives," *J. Geophys. Res.*, pp. 7209–7225, 1996.
- [2] M. J. Fennessey and J. Shukla, "Impact of initial soil wetness on seasonal atmospheric prediction," *J. Climate*, vol. 12, pp. 3167–3180, 1999.
- [3] R. D. Koster and M. J. Suarez, "A simple framework for examining the interannual variability of land surface moisture fluxes," *J. Climate*, vol. 12, pp. 1911–1917, 1999.
- [4] R. J. Oglesby, "Springtime soil moisture, natural climate variability and North American drought as simulated by the NCAR community model 1," *J. Climate*, vol. 4, pp. 890–897, 1991.
- [5] T. J. Schmugge, "Applications of passive microwave observations of surface soil moisture," *J. Hydrol.*, vol. 213, pp. 188–197, 1998.
- [6] T. J. Jackson, D. M. Le Vine, A. Y. Hsu, A. Oldak, P. J. Starks, C. T. Swift, J. D. Isham, and M. Haken, "Soil moisture mapping at regional scales using microwave radiometry: The Southern Great Plains Hydrology Experiment," *IEEE Trans. Geosci. Remote Sensing*, vol. 37, pp. 2136–2151, Sept. 1999.
- [7] J.-P. Wigneron, P. Waldteufel, A. C. Chanzy, J.-C. Calvet, and Y. H. Kerr, "Two-dimensional microwave interferometer retrieval capabilities over land surfaces (SMOS mission)," *Remote Sens. Environ.*, vol. 73, pp. 270–282, 2000.
- [8] E. J. Burke, R. J. Gurney, L. P. Simmonds, and T. J. Jackson, "Calibrating a soil water and energy budget model with remotely sensed data to obtain quantitative information about the soil," *Water Resources Res.*, vol. 33, pp. 1689–1697, 1997.
- [9] Y. H. Kerr, P. Waltuefel, J.-P. Wigneron, J.-M. Martinuzzi, J. Font, and M. Berger, "Soil moisture retrieval from space: The Soil Moisture and Ocean Salinity (SMOS)," *IEEE Trans. Geosci. Remote Sensing*, vol. 39, pp. 1729–1735, Aug. 2001.
- [10] M. Drusch, E. F. Wood, and C. Simmer, "Up-scaling effects in passive microwave remote sensing: ESTAR 1.4 GHz measurements during SGP '97," *Geophys. Res. Lett.*, vol. 26, pp. 879–882, 1999.
- [11] Y. A. Liou, E. J. Kim, and A. W. England, "Radiobrightness of prairie soil and grassland during dry-down simulations," *Radio Sci.*, vol. 33, pp. 259–265, 1998.
- [12] W. T. Crow, M. Drusch, and E. F. Wood, "An observation system simulation experiment for the impact of land surface heterogeneity on AMSR-E soil moisture," *IEEE Trans. Geosci. Remote Sensing*, vol. 39, pp. 1622–1631, Aug. 2001.
- [13] A. A. Van de Griend, J.-P. Wigneron, and P. Waldteufel, "Parameter retrieval of inhomogeneous surfaces using 1.4 GHz multi-angle brightness temperature observations," *IEEE Trans. Geosci. Remote Sensing*, vol. 41, pp. 803–811, Apr. 2003.
- [14] X. B. Zeng, M. Shaikh, Y. J. Dai, R. E. Dickinson, and R. Myneni, "Coupling of the common land model to the NCAR community climate model," *J. Climate*, vol. 15, pp. 1832–1854, 2002.
- [15] G. B. Bonan, "A land surface model [LSM version 1.0] for ecological, hydrological, and atmospheric studies: Technical description and user's guide," NCAR, Boulder, CO, Tech. Note NCAR/TN-417+STR, 1996.
- [16] R. E. Dickinson, A. Henderson-Sellers, P. J. Kennedy, and M. F. Wilson, "Biosphere-atmosphere transfer scheme [BATS] for the NCAR community climate model," NCAR, Boulder, CO, Tech. Note NCAR/TN-275+STR, 1986.
- [17] Y. J. Dai and Q. C. Zeng, "A land surface model [IAP94] for climate studies, I: Formulation and validation in off-line experiments," *Adv. Atmos. Sci.*, vol. 14, pp. 433–460, 1997.
- [18] P. G. Jarvis, "Interpretation of variations in leaf water potential and stomatal conductance found in canopies in field," *Phil. Trans. R. Soc. London B*, vol. 273, pp. 593–601, 1976.
- [19] K. Mitchell, C. Marshall, D. Lohmann, M. Ek, Y. Lin, P. Grunmann, P. Houser, E. Wood, J. Schaake, D. Lettenmaier, D. Tarpley, W. Higgins, R. Pinker, A. Robock, B. Cosgrove, J. Entin, and Q. Duan, "The collaborative GCIIP Land Data Assimilation (LDAS) project and supportive NCEP uncoupled land-surface modeling initiatives," in *Proc. 15th Amer. Meteorological Soc. Conf. Hydrology*, 2000.
- [20] P. J. Camillo, P. E. O'Neill, and R. J. Gurney, "Estimating soil hydraulic parameters using passive microwave data," *IEEE Trans. Geosci. Remote Sensing*, vol. GE-24, pp. 930–936, Nov. 1986.
- [21] M. C. Dobson, F. T. Ulaby, M. T. Hallikainen, and M. A. El-Rayes, "Microwave behavior of wet soil, 2: Dielectric mixing models," *IEEE Trans. Geosci. Remote Sensing*, vol. GE-23, pp. 35–46, Jan. 1985.
- [22] T. T. Wilheit, "Radiative transfer in a plane stratified dielectric," *IEEE Trans. Geosci. Electron.*, vol. GE-16, pp. 138–143, 1978.
- [23] T. J. Jackson and T. J. Schmugge, "Vegetation effects on the microwave emission of soils," *Remote Sens. Environ.*, vol. 36, pp. 203–212, 1991.
- [24] A. A. Van de Griend and J.-P. Wigneron, "The b factor as a function of frequency and canopy type at H-polarization," *IEEE Trans. Geosci. Remote Sensing*, vol. 42, pp. 786–794, Apr. 2004.
- [25] Q. Y. Duan, S. Sorooshian, and V. K. Gupta, "Optimal use of the SCE-UA global optimization method for calibrating watershed models," *J. Hydrol.*, vol. 158, pp. 265–284, 1994.
- [26] T. Pellarin, J.-P. Wigneron, J.-C. Calvet, M. Berger, H. Douville, P. Ferrazzoli, Y. H. Kerr, E. Lopez-Baeza, J. Pulliainen, L. P. Simmonds, and P. Waldteufel, "Two-year global simulation of L-band brightness temperatures over land," *IEEE Trans. Geosci. Remote Sensing*, vol. 41, pp. 2135–2139, Sept. 2003.
- [27] E. J. Burke and L. P. Simmonds, "Effects of sub-pixel heterogeneity on the retrieval of soil moisture from passive microwave radiometry," *Int. J. Remote Sens.*, vol. 24, pp. 2085–2104, 2003.

Eleanor J. Burke, photograph and biography not available at the time of publication.

W. James Shuttleworth, photograph and biography not available at the time of publication.

Paul R. Houser, photograph and biography not available at the time of publication.